

23. H. Lin, A. C. Spradling, *Development* **124**, 2463 (1997).  
 24. M. Parisi, H. Lin, *Genetics* **153**, 235 (1999).  
 25. D. Chen, D. M. McKeearin, *Curr. Biol.* **13**, 1786 (2003).  
 26. X. Song et al., *Development*, **131**, 1343 (2004).  
 27. We thank R. Wharton for Nos-Myc flies and nos

cDNA. B. Hogan and the Lin Lab members provided valuable comments. This work was supported by NIH (HD33760).

**Supporting Online Material**  
[www.sciencemag.org/cgi/content/full/1093983/DC1](http://www.sciencemag.org/cgi/content/full/1093983/DC1)  
 Materials and Methods

Figs. S1 and S2  
 References

24 November 2003; accepted 9 February 2004  
 Published online 19 February 2004;  
 10.1126/science.1093983  
 Include this information when citing this paper.

# Envelope-Constrained Neutralization-Sensitive HIV-1 After Heterosexual Transmission

Cynthia A. Derdeyn,<sup>1,7</sup> Julie M. Decker,<sup>3</sup>  
 Frederic Bibollet-Ruche,<sup>2,7</sup> John L. Mokili,<sup>4</sup> Mark Muldoon,<sup>5</sup>  
 Scott A. Denham,<sup>1</sup> Marantha L. Heil,<sup>1</sup> Francis Kasolo,<sup>8</sup>  
 Rosemary Musonda,<sup>9</sup> Beatrice H. Hahn,<sup>1,2,7</sup>  
 George M. Shaw,<sup>1,2,3,7</sup> Bette T. Korber,<sup>4,10</sup> Susan Allen,<sup>6,7</sup>  
 Eric Hunter<sup>1,7\*</sup>

Heterosexual transmission accounts for the majority of human immunodeficiency virus-1 (HIV-1) infections worldwide, yet the viral properties that determine transmission fitness or outgrowth have not been elucidated. Here we show, for eight heterosexual transmission pairs, that recipient viruses were monophyletic, encoding compact, glycan-restricted envelope glycoproteins. These viruses were also uniquely sensitive to neutralization by antibody from the transmitting partner. Thus, the exposure of neutralizing epitopes, which are lost in chronic infection because of immune escape, appears to be favored in the newly infected host. This reveals characteristics of the envelope glycoprotein that influence HIV-1 transmission and may have implications for vaccine design.

The acquired immunodeficiency syndrome (AIDS) pandemic has arisen largely through heterosexual transmission of HIV-1, yet the frequency of infection per coital act is less than 0.5% (1). This inefficiency could reflect low amounts of virus inoculum, restricted access to target cells, selective transmission, or outgrowth of a subset of viruses. Studies of mother-to-infant transmission first demonstrated that a restricted subset of viruses was observed soon after infection (2). Limited studies of sexual transmission have demonstrated that homogeneous, macrophage-tropic virus strains generally establish infection (3–6), although more recent analyses have suggested that greater genotypic complexity may

be present after sexual transmission than was previously appreciated (7, 8). None of these studies has systematically examined the properties of the virus in a series of male-to-female (MTF) and female-to-male (FTM) transmission pairs. We examined a cohort of HIV-discordant cohabiting couples in Zambia to determine the nature of heterosexually acquired HIV-1 infection.

Eight heterosexual transmission pairs were studied, all derived from a larger cohort of over 1000 couples in Lusaka, Zambia (9, 10). Participation in this prospective epidemiological study included preventative counseling and monitoring for seroconversion at 3-month intervals (11). Despite a demonstrated reduction in transmission rate, seroconversion occurred at a frequency of 8.5 per 100 person years and was similar for MTF and FTM transmissions (12). Eighty-seven percent of transmission events were epidemiologically linked, indicating that these were predominantly monogamous relationships (13). This cohort therefore provided a setting in which to examine virologic determinants of heterosexual HIV-1 transmission in Africa.

Blood samples were collected simultaneously from both donor and recipient of four MTF and four FTM transmission pairs within 3 to 4 months of the last seronegative blood test of the recipient. These pairs represented transmission occurring in both directions,

with broad variation in the time to transmission after enrollment, the viral load of the donors, and the early viral load of the recipients (table S1). For each transmission pair, either full-length (gp160) or partial (gp120, loops V1 to V5) *env* gene sequences were amplified from uncultured peripheral blood mononuclear cell (PBMC) DNA. Viral sequences from plasma were also included for five of the donors and two of the recipients. A neighbor-joining tree was constructed with 291 nucleotide sequences [spanning nucleotides 457 to 1254 relative to the HXB2 reference strain gp160 coding region (14)] from the eight transmission pairs (11). These were combined with 79 reference sequences from the HIV Sequence Database, including representatives of all group M clades and 50 clade C sequences (15). Clear epidemiologic linkage was apparent for each transmission pair (Fig. 1), with no evidence of contamination or intersubtype recombination within the sequences (fig. S1). Sequences from seven of the eight pairs clustered with subtype C reference strains, whereas sequences from pair 71 were more closely related to subtype G. The subtype C donor-recipient sequences from Zambia intermingled with subtype C sequences from other regions, confirming the difficulty of classifying subtype C sequences on a geographic basis (16). In all cases, the recipient sequences formed a distinct subcluster with high bootstrap support within the framework of the donor sequences.

To better examine the evolutionary relationships of donor and recipient sequences, maximum likelihood (ML) trees for each transmission pair were constructed from 257 nucleotide sequences spanning positions 391 to 1254 of the HXB2 gp160 coding region (11). To enable statistical analyses, only sequences that completely spanned the loops V1 to V4 were included in this and all subsequent analyses. Examination of each tree revealed that an extreme bottleneck occurred during both MTF and FTM transmission (Fig. 2). A Wilcoxon comparison of branch lengths to the ancestral node for donor and recipient sequences confirmed that limited divergence had occurred after transmission as compared to that of the donor quasispecies ( $P < 0.0001$ ). In all cases, a distinct subcluster of recipient sequences was found, although in one case (pair 109) four highly related donor sequences were embedded among the recipient sequences (Fig. 2). These data argue for transmission or outgrowth of a single sequence from the donor quasispecies. However,

<sup>1</sup>Department of Microbiology, <sup>2</sup>Department of Medicine, <sup>3</sup>Howard Hughes Medical Institute, University of Alabama at Birmingham, Birmingham, AL 35294, USA. <sup>4</sup>HIV Sequence Database, Los Alamos National Laboratory, Los Alamos, NM 87544, USA. <sup>5</sup>Department of Mathematics, University of Manchester Institute of Science and Technology, Manchester, UK. <sup>6</sup>Department of Epidemiology and International Health, School of Public Health; <sup>7</sup>University of Alabama at Birmingham Center for AIDS Research; University of Alabama at Birmingham, Birmingham, AL 35294, USA. <sup>8</sup>Department of Pathology and Microbiology, University Teaching Hospital, Lusaka, Zambia. <sup>9</sup>Tropical Disease Research Center, Ndola, Zambia. <sup>10</sup>Santa Fe Institute, Santa Fe, NM 87501, USA.

\*To whom correspondence should be addressed. E-mail: ehunter@uab.edu

REPORTS

er, given the intrinsic limitations of sampling, we cannot distinguish between a true transmission bottleneck, transmission of the predominantly replicating form in genital tissues, or transmission of multiple forms followed by outgrowth of a particular variant.

Inspection of each donor-recipient pair suggested that recipient envelope (Env) glycoproteins contained shorter variable loops than the majority of those in the donor quasispecies (17). Using the null hypothesis that the recipient is equally likely to receive any sequence from the donor

pool, the length (from the first cysteine in V1 to the end of V4) was determined for each donor sequence (11). The frequency of sequences below, at, or above the median donor length was then determined and compared to recipient sequences in a nonparametric test (Fig. 3A). Six of the eight pairs had recipient sequences in which the lengths of V1 to V4 were below the donor median. Given the frequency and distribution of the donor lengths, this observation was highly significant when the eight pairs were considered together ( $P = 0.013$ ). The

significance was confirmed independently using a one-sided Wilcoxon test ( $P = 0.03$ ), which considered the relative ranking of the recipient compared to the set of sequences in the donor. Using a two-sided Wilcoxon test, the lengths of V1 to V4 of the eight recipient sequences were found to differ significantly from the subtype C V1 to V4 sequences currently in the HIV Database ( $n = 50$ , including only one sequence per individual;  $P = 0.02$ ). By contrast, no significant difference was observed for median lengths of the sequences of V1 to V4 from each of the eight donors as compared to the database. Taken together, these results argue that viruses encoding Env glycoproteins with shorter V1-V4 regions are transmitted or grow out in recipients with a frequency significantly greater than would be expected by chance.

Because changes in length that occur within V1, V2, and V4 often involve the addition or loss of N-linked glycosylation (N-gly) sites, we applied a similar analysis to the number of N-gly sites within the sequence of V1 to V4 (Fig. 3B). Five of the eight pairs had recipient sequences that contained less than the median number of N-gly sites in the donor, and this observation again reached significance when the pairs were considered in aggregate ( $P = 0.037$ ). In contrast to V1-V4 length, neither the recipient nor the donor V1-V4 region differed significantly from the database of subtype C viruses in the distribution of the number of N-gly sites.

Structural predictions place the V1V2 loop near a  $\beta$  sheet that modulates gp120 interactions with CD4 and a coreceptor (18–20). The V4 loop is predicted to lie on the outer domain of the gp120 trimer, and changes in its size can influence the packing and orientation of surrounding glycans, which are proximal to the CD4 binding site (21). Thus, a likely functional consequence of having a compact V1-V4 region is increased exposure of the CD4 binding domain, a feature that is often accompanied by enhanced susceptibility to neutralization (22–25). We therefore examined this property using virions that were pseudotyped with donor- and recipient-derived Env glycoproteins from five of the transmission pairs. To do this, a single-round infection assay was used to test the ability of linked donor plasma and a heterologous plasma pool from 15 unrelated subtype C-infected individuals in Lusaka to neutralize virions pseudotyped with donor and recipient Env glycoproteins (11, 26–29).

Neutralization profiles demonstrated that the recipient pseudotypes were as much as 10 times more sensitive to neutralization by linked donor plasma than the donor pseudotypes, as shown for transmission pair 135 (Fig. 4A). To more broadly define the donor-recipient differences in neutralization sensitivity, an analysis similar to that described for V1-V4 length and glycosylation

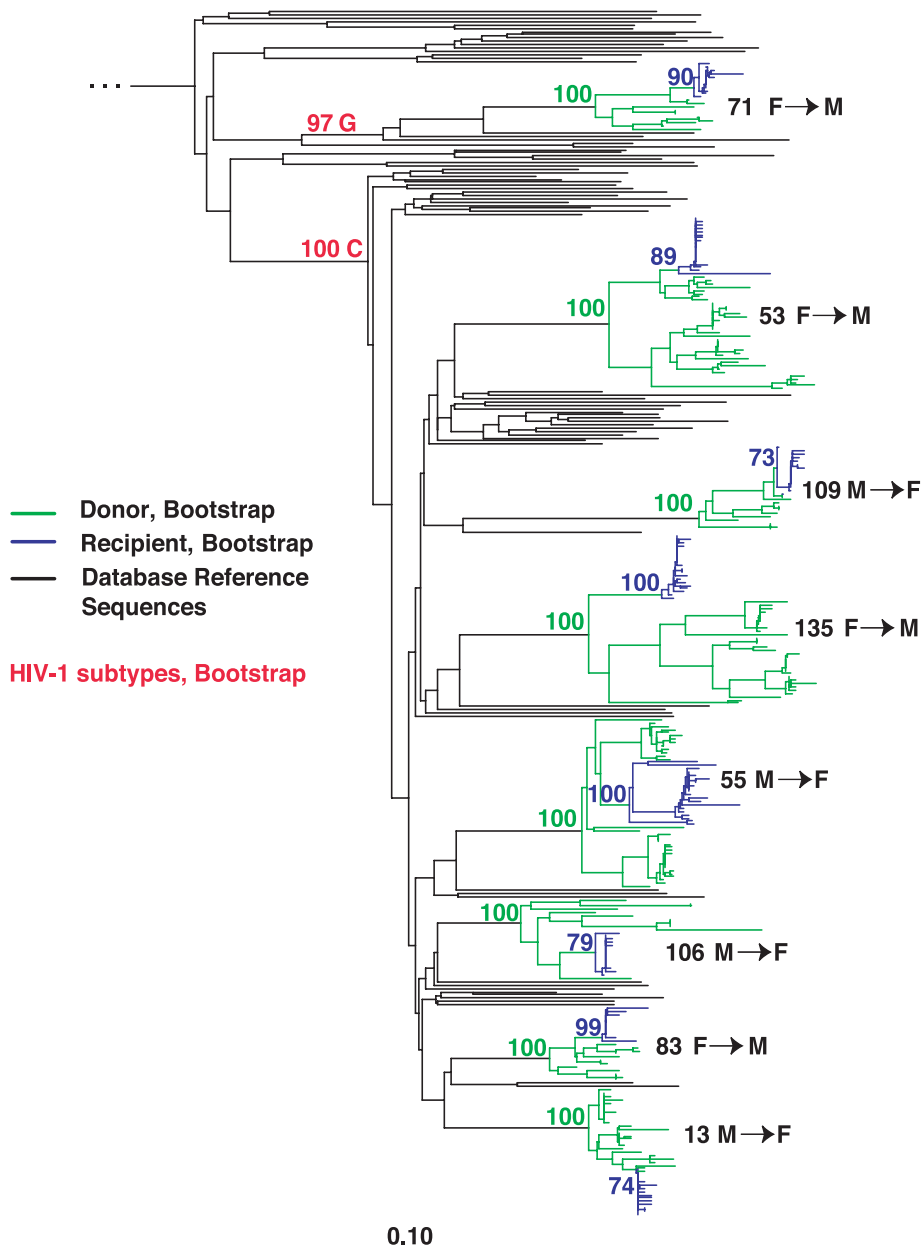


**Fig. 1.** Neighbor-joining tree. Nucleotide sequences from donors (green) and recipients (blue) were aligned and subjected to phylogenetic tree construction using the F84 evolutionary model. Reference strains from group M HIV-1 are indicated in black. Two reference sequences (UCD83003 and UCD90121) were used as an outgroup. Horizontal branch lengths are drawn to scale, with the bar representing 10% divergence. Bootstrap values are indicated to the left of the node. M→F, MTF transmission; F→M, FTM transmission.

was applied to neutralization by antibodies in donor and pooled plasma. All five recipients analyzed harbored Env glycoproteins that were neutralized by donor plasma with median inhibitory concentration ( $IC_{50}$ ) values below that of the donor (Fig. 4B), and this result was highly significant when the pairs were considered in aggregate ( $P = 0.013$ ). Moreover, Fig. 4C demonstrates a strong correlation between sensitivity to donor and pooled plasma and illustrates the high sensitivity of the recipient Env glycoproteins to neutralization by antibody from both sources. In contrast, the donor Env glycoproteins displayed a broad range of susceptibility to neutralization. Despite this observation, the difference in sensitivity to neutralization by pooled plasma between donor and recipient did not reach significance on a pair-by-pair basis (fig. S2). These data demonstrate that viruses that are successful in establishing new infections via heterosexual transmission have a neutralization profile that includes sensitivity to antibodies in the infecting partner's plasma.

This analysis of HIV-1 Env glycoproteins in eight African heterosexual transmission pairs reveals an extreme bottleneck for both MTF and FTM transmission. Shorter V1-V4 length, fewer glycans, and a greater susceptibility to neutralization of recipient Env glycoproteins suggest that transmission or outgrowth selects for envelope conformations with more accessible receptor-binding domains. In support of this idea, the V1V2 region has been shown to modulate utilization of CD4 and virus susceptibility to antibody neutralization (25, 30, 31). Thus, it is most likely that the viruses that ultimately establish infection through heterosexual contact are more fit in their interaction with a particular cell type than others in the donor quasispecies.

In individuals chronically infected with HIV-1 and the simian immunodeficiency virus, cell-free virus is under significant selection pressure from neutralizing antibodies (29, 32–36). Our results suggest that the acquisition of resistance to antibody neutralization has a fitness cost in terms of transmission, or in terms of establishing de novo infection, that could be exploited in vaccine design. In particular, the enhanced sensitivity of the variants to neutralization that was observed soon after infection raises the possibility that lower titers of vaccine-induced neutralizing antibodies than have been considered to date may provide protection against infection through heterosexual contact. Even assuming that multiple forms are generally transmitted, a vaccine-primed neutralizing response may still confer a protective benefit on newly infected individuals. These questions notwithstanding, the findings reported here open new avenues of investigation aimed at a better understanding of HIV-1 transmission and the rational design of effective vaccines.

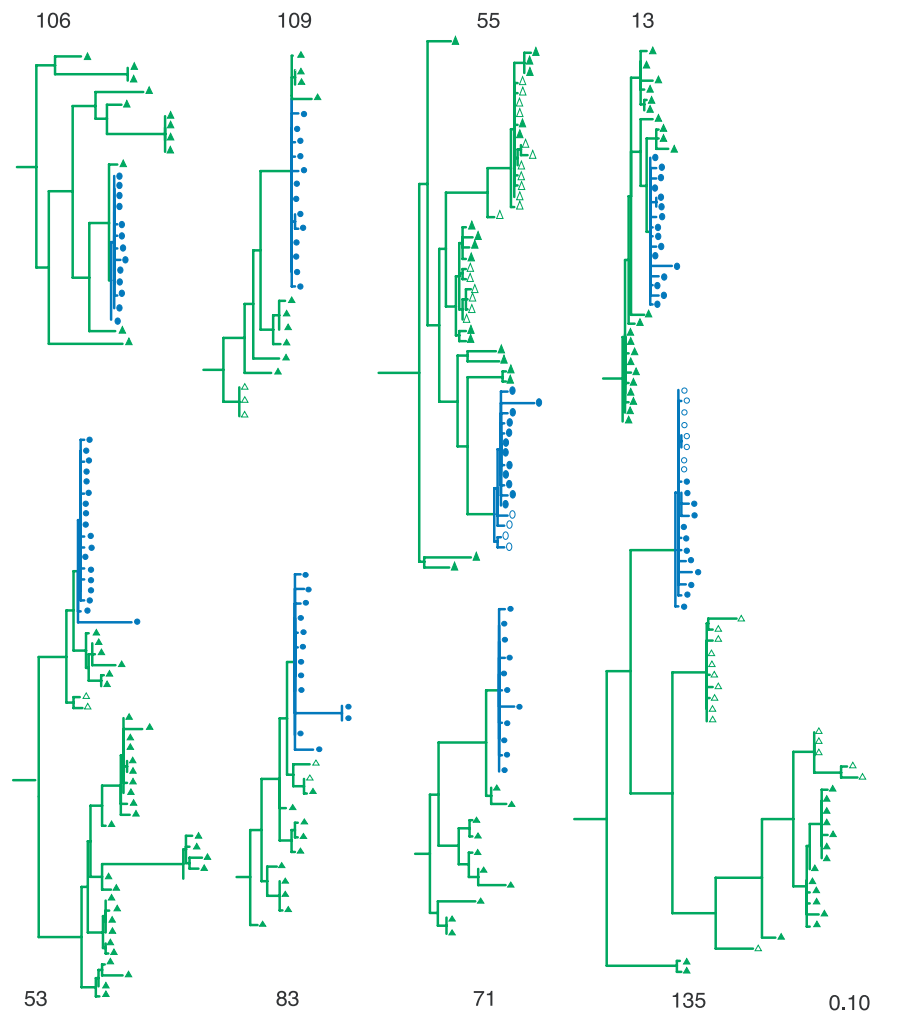


**Fig. 2.** Maximum likelihood analysis. Nucleotide sequences from donors (green triangles) and recipients (blue circles) were subjected to maximum likelihood analysis. Horizontal branch lengths are drawn to scale, with the bar representing 10% divergence. Solid symbols represent sequences derived from uncultured PBMC DNA; open symbols represent those derived from plasma.

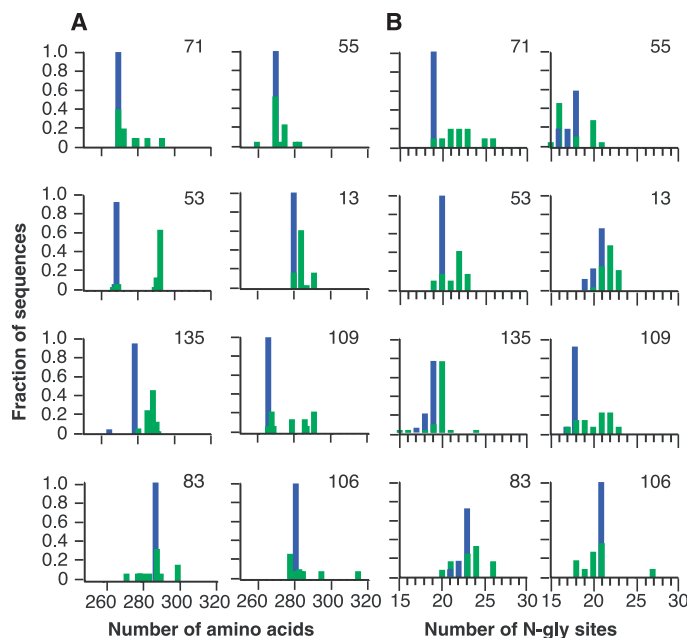


**Fig. 3.** V1-V4 length and number of N-gly sites in donor and recipient sequences. The number of (A) amino acids or (B) N-gly sites in V1-V4 is plotted along the horizontal axes. The fraction of donor (green) or recipient (blue) sequences with a given value is shown on the vertical axes. Because the transmitted sequences tend to be short relative to their own donor's quasispecies, it was not feasible to combine all donor and recipient sequences into a single comparison.

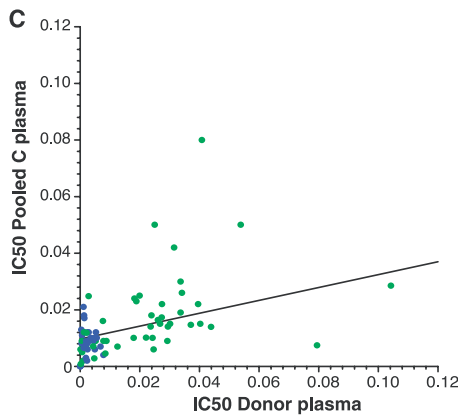
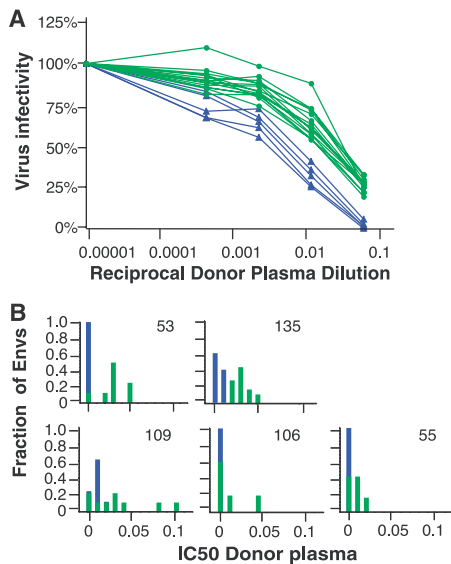


**Fig. 4.** Neutralization by donor and pooled subtype C plasma. **(A)** Neutralization profile of plasma-derived donor (green) and recipient (blue) Env pseudotypes from transmission pair 135 by donor plasma. Virus infectivity, as a percentage of the control, is plotted along the vertical axis. The reciprocal of the plasma dilution is graphed along the horizontal axis on a log<sub>10</sub> scale. Each curve represents the sensitivity to neutralization of an individual Env pseudotype. **(B)** The distribution of neutralization sensitivity for donor (green) and recipient (blue) Env pseudotypes for five transmission pairs, with IC<sub>50</sub> values for donor plasma (rounded to the nearest two-digit value) plotted on the horizontal axis. The fraction of Env pseudotypes with a given IC<sub>50</sub> is indicated on the vertical axis. **(C)** Linear regression analysis of neutralization by donor (horizontal axis) and pooled (vertical axis) plasma for donor (green) and recipient (blue) Env pseudotypes (*R*-squared value = 0.23; *P* value = 0.00002; slope = 0.31, standard error = 0.07). The number of Env pseudotypes evaluated was 106 (5 donor and 7 recipient), 109 (8 donor and 3 recipient), 135 (14 donor and 5 recipient), 55 (12 donor and 8 recipient), and 53 (6 donor and 3 recipient).

neutralization is graphed along the horizontal axis on a log<sub>10</sub> scale. Each curve represents the sensitivity to neutralization of an individual Env pseudotype. **(B)** The distribution of neutralization sensitivity for donor (green) and recipient (blue) Env pseudotypes for five transmission pairs, with IC<sub>50</sub> values for donor plasma (rounded to the nearest two-digit value) plotted on the horizontal axis. The fraction of Env pseudotypes with a given IC<sub>50</sub> is indicated on the vertical axis. **(C)** Linear regression analysis of neutralization by donor (horizontal axis) and pooled (vertical axis) plasma for donor (green) and recipient (blue) Env pseudotypes (*R*-squared value = 0.23; *P* value = 0.00002; slope = 0.31, standard error = 0.07). The number of Env pseudotypes evaluated was 106 (5 donor and 7 recipient), 109 (8 donor and 3 recipient), 135 (14 donor and 5 recipient), 55 (12 donor and 8 recipient), and 53 (6 donor and 3 recipient).

16. B. Gaschen *et al.*, *Science* **296**, 2354 (2002).
17. C. A. Derdeyn, E. Hunter, unpublished observations.
18. C. D. Rizzuto *et al.*, *Science* **280**, 1949 (1998).
19. P. D. Kwong *et al.*, *Nature* **393**, 648 (1998).
20. P. D. Kwong *et al.*, *Struct. Fold. Design* **8**, 1329 (2000).
21. P. D. Kwong, personal communication.
22. P. Kolchinsky, E. Kiprilov, J. Sodroski, *J. Virol.* **75**, 2041 (2001).
23. B. A. Puffer *et al.*, *J. Virol.* **76**, 2595 (2002).
24. T. G. Edwards *et al.*, *J. Virol.* **75**, 5230 (2001).
25. W. E. Johnson *et al.*, *J. Virol.* **76**, 2075 (2002).
26. C. A. Derdeyn *et al.*, *J. Virol.* **74**, 8358 (2000).
27. C. A. Derdeyn *et al.*, *J. Virol.* **75**, 8605 (2001).
28. X. Wei *et al.*, *Antimicrob. Agents Chemother.* **46**, 1896 (2002).
29. X. Wei *et al.*, *Nature* **422**, 307 (2003).
30. P. Kolchinsky, E. Kiprilov, P. Bartley, R. Rubinstein, J. Sodroski, *J. Virol.* **75**, 3435 (2001).
31. A. Ly, L. Stammatos, *J. Virol.* **74**, 6769 (2000).
32. D. D. Richman, T. Wrin, S. J. Little, C. J. Petropoulos, *Proc. Natl. Acad. Sci. U.S.A.* **100**, 4144 (2003).
33. M. Arendrup *et al.*, *J. Acquir. Immune Defic. Syndr.* **5**, 303 (1992).
34. J. Albert *et al.*, *AIDS* **4**, 107 (1990).
35. A. P. Bradney, S. Scheer, J. M. Crawford, S. P. Buchbinder, D. C. Montefiori, *J. Infect. Dis.* **179**, 1264 (1999).
36. B. Chackerian, L. M. Rudensey, J. Overbaugh, *J. Virol.* **71**, 7719 (1997).
37. We thank the participants, staff, and Project Management Group of the Lusaka cohort; P. Sharp and P. Kwong for discussion; J. Coffin and J. L. Blackwell for critiques; J. Lee and D. -T. Chen for statistical analyses; K. Yusim for phylogenetic analyses; and M. Salazar [University of Alabama at Birmingham (UAB) Center for AIDS Research (CFAR) DNA Sequence Analysis Core, P30-AI-27767] and K. Zscheck (Lone Star Labs) for technical assistance. Virus culture was performed in the UAB CFAR Central Virus Core (P30-AI-27767). This work was supported by NIH grants AI-51231 (E.H.), AI-40951 (S.A.), U01-AI-41530 (G.S. and B.H.), N01-85338 (B.K.), and amfAR (American Foundation for AIDS Research) 70530-28-RFV (C.D.).

**References and Notes**

1. P. Piot, M. Bartos, P. D. Ghys, N. Walker, B. Schwartzlander, *Nature* **410**, 968 (2001).
2. S. M. Wolinsky *et al.*, *Science* **255**, 1134 (1992).
3. T. Zhu *et al.*, *Science* **261**, 1179 (1993).
4. T. Zhu *et al.*, *J. Virol.* **70**, 3098 (1996).
5. T. F. Wolfs, G. Zwart, M. Bakker, J. Goudsmit, *Virology* **189**, 103 (1992).
6. A. B. van't Wout *et al.*, *J. Clin. Invest.* **94**, 2060 (1994).
7. E. M. Long *et al.*, *Nature Med.* **6**, 71 (2000).
8. G. H. Learn *et al.*, *J. Virol.* **76**, 11953 (2002).
9. S. L. McKenna *et al.*, *AIDS* **11** (suppl. 1), S103 (1997).
10. S. Allen *et al.*, *AIDS* **17**, 733 (2003).
11. Materials and methods are available as supporting material on Science Online.
12. U. S. Fideli *et al.*, *AIDS Res. Hum. Retroviruses* **17**, 901 (2001).
13. S. Trask *et al.*, *J. Virol.* **76**, 397 (2002).
14. See the sequence locator tool at www.hiv.lanl.gov.
15. *HIV Sequence Compendium*, C. Kuiken, B. Foley, E. Freed, B. Hahn, P. A. Marx, F. McCutchan, J. Mellors, S. Wolinsky, B. Korber, Eds. (Theoretical Biology and Biophysics Group, Los Alamos National Laboratory, Los Alamos, NM, 2002).

**Supporting Online Material**

www.sciencemag.org/cgi/content/full/303/5666/2019/DC1  
 Materials and Methods  
 Figs. S1 to S3  
 Table S1  
 References

30 October 2003; accepted 4 February 2004

# A MicroRNA as a Translational Repressor of APETALA2 in Arabidopsis Flower Development

Xuemei Chen

Plant microRNAs (miRNAs) show a high degree of sequence complementarity to, and are believed to guide the cleavage of, their target messenger RNAs. Here, I show that miRNA172, which can base-pair with the messenger RNA of a floral homeotic gene, *APETALA2*, regulates *APETALA2* expression primarily through translational inhibition. Elevated miRNA172 accumulation results in floral organ identity defects similar to those in loss-of-function *apetala2* mutants. Elevated levels of mutant *APETALA2* RNA with disrupted miRNA172 base pairing, but not wild-type *APETALA2* RNA, result in elevated levels of APETALA2 protein and severe floral patterning defects. Therefore, miRNA172 likely acts in cell-fate specification as a translational repressor of *APETALA2* in *Arabidopsis* flower development.

MicroRNAs (miRNAs), ~22-nucleotide non-coding RNAs that regulate protein-coding RNAs, are processed from longer hairpin

transcripts by the enzyme Dicer [reviewed in (1, 2)]. In *Arabidopsis*, the accumulation of miRNAs requires a Dicer homolog, DCL1,

and a novel protein, HEN1 [reviewed in (3)]. The two founding members of *Caenorhabditis elegans* miRNAs, *lin-4* and *let-7*, inhibit the translation of their target mRNAs through imperfect base-pairing interactions with their targets (4, 5). *Arabidopsis* miRNAs show a higher degree of sequence complementarity to their potential targets, and, like short interfering RNAs, several plant miRNAs direct the cleavage of their target RNAs (6–9). Here, I report the role of an *Arabidopsis* miRNA, miRNA172, in the control of floral organ identity and floral stem cell proliferation as a potential translational repressor of a floral homeotic gene.

Four organ types are specified in the floral meristem by the combinatorial actions of three classes of transcription factors, the floral A, B, and C genes [reviewed in (10)]. *APETALA2* (*AP2*, a class A gene) and

Waksman Institute, Rutgers University, Piscataway, NJ 08854, USA. E-mail: xuemei@waksman.rutgers.edu